Catastrophe and Stability Analysis of a Cable-Driven Actuator

James S. Sulzer, Michael A. Peshkin and James L. Patton

Abstract— **Recent work in human-robot interaction has revealed the need for compliant, human-friendly devices. One such device, known as the MARIONET, is a cable-driven single joint actuator with the intended applications of physical rehabilitation and assistive devices. In this work, the stability of the nonlinear system is determined in regards to its equilibria in a wide variety of configurations. In certain configurations, the canonical version of this mechanism experiences an interesting mathematical behavior known as "catastrophes". This behavior may be disadvantageous toward control or even safety. Several cases are thoroughly investigated, two cases where each of two degrees of freedom loses control, and the final case explores the use of a mechanical advantage such as a block and tackle. The study concludes that for a range of design options, the MARIONET does not suffer from any catastrophes. However, the unique behaviors such as a unidirectional bifurcation produced by certain configurations may have use outside of our objectives, perhaps as a type of switch or valve.**

I. INTRODUCTION

Recently, there has been interest in the stability and activity of human-machine interface devices. One such mechanism is a novel joint actuator known as the MARIONET (Moment arm Adjustment for Remote Induction Of Net Effective Torque). This cable-driven joint uses the concept of moment arm manipulation to produce torque on a human elbow.

Torque in a cable-driven joint is the cross-product of the tension in the cable and the moment arm it exerts on the joint. One may either increase the tension in order to alter torque, or manipulate the moment arm. Using the latter method, we chose to manipulate the moment arm in a rotational manner centered about the joint. This paradigm has the advantages of global controllability, uniform stiffness properties and small geometry. Fig. 1 provides a canonical example of the single joint MARIONET exerting torque on the user's elbow.

In the canonical design of Fig. 1, a controlled disk (Rotator) drives the Pulley of zero diameter located at (R_P, ϕ). Traveling through the Pulley is an inelastic cable, originating from a point of constant tension T (Tensioner) at (R_T, ζ), and ending at the user's hand (Link) at (R_L, θ). The Rotator of the MARIONET (ϕ) is position-controlled. Typically, the

Tensioner keeps the tension of the cable at a constant value. The torque on the elbow is a function of the moment arm exerted by the length of cable from the Link to the Pulley (L_{LP}).

This paper will explore the equilibria of the MARIONET under several different conditions. The first condition considers where the Pulley is under position control (a non-backdrivable Rotator). It is determined that the Link in this case will converge to the Pulley position in every configuration except for minute singularities. The second condition simulates a loss of control of the Pulley with the user rigidly controlling the Link (backdrivable Rotator). It is found that in certain portions of the workspace, the Pulley will settle to either of two equilibria, neither posing any danger to the user. The final portion of the analysis takes the second condition and investigates the effects of using different mechanical advantages on L_{LP}. The mechanical advantage, physically realized as a block and tackle, can cause interesting motions in the Rotator known as "catastrophes" (defined below). These motions could potentially cause control issues, but at the level of mechanical advantage of the MARIONET, poses no threat. We conclude that while the MARIONET in its present state has virtually no instabilities in its workspace, the unique type of catastrophe described may be able to be used in other applications. The following work has been inspired by analysis on a very similar mechanism known as a *Zeeman Catastrophe Machine* [1], [2]. The Zeeman Machine experiences a specific type of *catastrophe*, defined as a large change in internal configuration caused by a small change in external circumstances. While in everyday life, the term "catastrophe" has a negative connotation, it can be used for many useful applications. Examples of catastrophes include ski boot latches, buttons on a keyboard, and even the freezing of water. A catastrophe may be thought of as
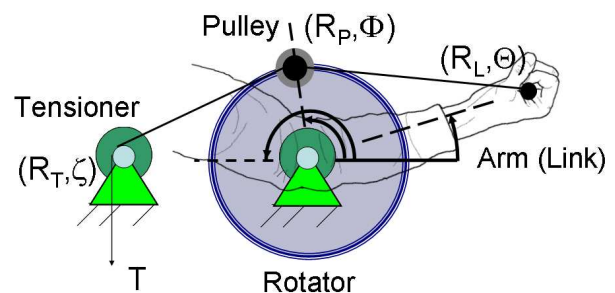

Fig. 1.   Schematic of canonical MARIONET.

a temporary instability while moving from one equilibrium state to another disconnected equilibrium. Since catastrophes depend on the equilibria of the mechanism, a quasistatic analysis of stability is necessary as opposed to other methods such as Lyapunov's Direct Method.

II. QUASISTATIC ANALYSIS OF EQUILIBRIA

In this section, quasistatic properties of the MARIONET are determined. There are two cases analyzed, one where the Rotator is under position control (non-backdrivable), and one where there is a loss of control of the Rotator (backdrivable) and the Link is under position control. The former part of the analysis begins looking at the energy of the mechanism, and then determines what geometrical factors allow it to converge to an equilibrium. The latter portion expands this finding to another degree of freedom as the Rotator is no longer rigidly controlled.

A. Non-backdrivable Rotator (ϕ is fixed)

Since the system is composed of a single, inelastic cable, the energy V, is a function of the change in length of the cable dx (excursion), and the tension T (assumed constant),

$$V = \int T dx. \tag{1}$$

The excursion of the cable is the difference of the total length and the original length l_0,

$$dx = L_{LP}(\theta, \phi) + L_{PT}(\phi, \zeta) - l_0, \tag{2}$$

where L_{LP} is the distance of the cable from the Pulley (R_P, ϕ) to the Link (R_L, θ), and L_{PT} is the distance from the Tensioner (R_T, ζ) to the Pulley found using geometry,

$$L_{LP} = \sqrt{R_L^2 + R_P^2 - 2R_L R_P \cos(\theta - \phi)}, \tag{3}$$

$$L_{PT} = \sqrt{R_P^2 + R_T^2 - 2R_P R_T \cos(\phi - \zeta)}. \tag{4}$$

The torque seen by the arm τ_E is the partial derivative of the energy with respect to θ:

$$\tau_E = \frac{\partial V}{\partial \theta} = \frac{R_L R_P}{L_{LP}} \sin(\theta - \phi) T, \tag{5}$$

The endpoint stiffness seen by the Link is the partial derivative of the torque with respect to θ:

$$k_E = \frac{\partial \tau_E}{\partial \theta} = \frac{R_L R_P}{L_{LP}} \cos(\theta - \phi) T$$
$$- \frac{R_L^2 R_P^2}{L_{LP}^3} \sin^2(\theta - \phi) T. \tag{6}$$

Therefore in this case, the equilibrium will be where $\theta - \phi = 0$, or more simply, the Link is attracted to the Pulley. The stiffness k_E determines the concavity of this energy relationship. This quantity is not always positive; the area where k_E is positive is defined as the *Region of Convergence* (Fig. 2). The region depends on the geometry of the device, and more specifically, the ratio between R_L and R_P. Its boundary represents the maximum torque exerted on the elbow for the domain of R_L:R_P. The upper portion
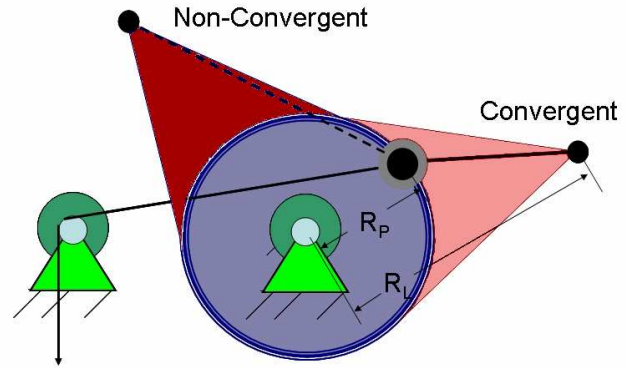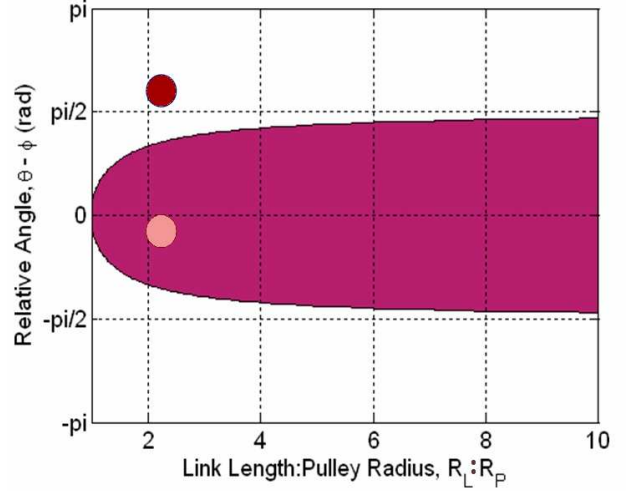

Fig. 2. (Above) Region of Convergence of Link relative to Pulley position with respect to geometry. This region represents the space where k_E is positive. (Below) Two configurations are shown, in the first (pink triangle), the Pulley is within the Region of Convergence (shown as a pink dot above), and in the second, the Pulley is now outside the Region of Convergence, also indicated above. For a non-backdrivable, position-controlled Rotator, the Region of Convergence indicates the most efficient workspace since it describes the extent of the maximum torque.

of the figure shows two locations that correspond to the colored triangles in the mechanism configuration below. These triangles represent the locus of Pulley locations that will be inside the Region of Convergence. Note that the boundaries approach $\theta - \phi = \pm\frac{\pi}{2}$ as the ratio R_L:R_P increases. Contrary to the name of the region, almost all states of θ will result in an eventual convergence to an equilibrium at ϕ in the non-backdrivable Rotator case, an exception being where $\phi = \theta + \pi$, or in other words, where L_{LP} exerts zero moment arm on the joint. This region is important because it determines the range of operation that should be used for maximum torque in either direction. One may conclude from this information that at rest, the non-backdrivable case is inherently stable at all non-singular points in the workspace. The Region of Convergence gains even more relevance in the next section, where the Rotator is backdrivable.

B. Backdrivable Rotator

While the Region of Convergence for the non-backdrivable case only shows the region between the maximum torque

configurations, the situation changes when the ϕ has some degree of backdrivability, and there are two coupled regions. The following sections will explore this more interesting behavior, where the Pulley ϕ is left free to move, and the Link θ is controlled.

In this case, there are now two degrees of freedom to account for in the system, θ and ϕ. The torque seen by the Rotator τ_R is:

$$\tau_R = \frac{\partial V}{\partial \phi} = \frac{R_L R_P}{L_{LP}} \sin(\theta - \phi) T + \frac{R_P R_T}{L_{PT}} \sin(\phi - \zeta) T. \quad (7)$$

Note that this equation is similar to (5), with another term. These terms represent the contribution to torque made by L_{LP} and L_{PT}, respectively. This concept will become more important as more analysis is covered. The Rotator's stiffness is,

$$\frac{\partial \tau_R}{\partial \phi} = k_E + \frac{R_P R_T}{L_{PT}} \cos(\phi - \zeta) T - \frac{R_P{}^2 R_T{}^2}{L_{PT}{}^3} \sin^2(\phi - \zeta) T, \quad (8)$$

where the first term k_E is from (6), and the second two terms comprise the identical form of (6) but with different parameters, will be referred to as k_R.

Combining (7) with (5) total torque is expressed as,

$$[\tau_E, \tau_R] = \left[\frac{R_L R_P}{L_{LP}} \sin(\theta - \phi) T, \frac{R_L R_P}{L_{LP}} \sin(\theta - \phi) T + \frac{R_P R_T}{L_{PT}} \sin(\phi - \zeta) T \right], \quad (9)$$

and the total stiffness is,

$$\begin{bmatrix} \frac{\partial \tau_E}{\partial \theta} & \frac{\partial \tau_E}{\partial \phi} \\ \frac{\partial \tau_R}{\partial \theta} & \frac{\partial \tau_R}{\partial \phi} \end{bmatrix} = \begin{bmatrix} k_E & k_E \\ k_E & k_E + k_R \end{bmatrix}. \quad (10)$$

The characteristic equation for this matrix is,

$$\begin{bmatrix} \lambda - k_E & k_E \\ k_E & \lambda - k_E + k_R \end{bmatrix} = \lambda^2 - (2k_E + k_R)\lambda + k_E k_R = 0. \quad (11)$$

Thus, the eigenvalues λ of this matrix will be positive when both k_E and k_R are positive.

1) Convergent Behavior: Convergence will occur where both k_E and k_R are positive - which is inside their Regions of Convergence. Since the form of k_R identical to k_E, the Region of Convergence for k_R is looks identical to Fig. 2 except for different parameters (i.e. the vertical axis is $\phi - \zeta$, and the horizontal axis is $R_P : R_T$).

Where both k_E and k_R are positive, both degrees of freedom of the system share a common equilibrium (the system is convergent), as shown in the top configuration of Fig. 3. In this case, the colored triangles that represent the Region of Convergence for one section of cable overlaps the other. In physical terms, this means that the device has one position of minimum potential energy, $\zeta = \phi = \theta$. Hence,

when the Pulley is within both Regions of Convergence, the device is stable.

Fig. 4 is a representation of the minimum energy surface for multiple configurations of the MARIONET. This figure can be used to compare the configurations shown in Fig. 3 with their minimum potential energy, and thus the equilibria of the system. While the ratio of the Link length to Pulley radius ($R_L : R_P$) is variable, the ratio of the Pulley radius to the Tensioner distance ($R_P : R_T$) is fixed at an arbitrary value of 2 in this example. Note that both θ and ϕ are each S^1 projected on $\Re^1$. In this figure, there are two red "flaps" that protrude from a smoother, gray surface. The meaning behind these features will be discussed later in this section. In regards to convergent behavior, this workspace corresponds to the area on the minimum energy surface where θ is outside the region of the red flaps, typically where $|\theta| > \frac{\pi}{2}$. In this area there is a bijective relationship between θ and ϕ, meaning there is only one equilibrium point for each input.

2) Bifurcation: The system has a single equilibrium when the Regions of Convergence overlap, but as they move away from each other, the system reaches a singularity known as a bifurcation (see center configuration of Fig. 3). The bifurcation represents the configuration where both sides of the cable are exerting the maximum torque possible on the Pulley, and any further movement of the Link will pull the Pulley to one side or the other. In mathematical terms, this is where both k_R and k_E are zero.

The locus of bifurcation points is shown in the example given in Fig. 4, precisely where the red flaps protrude from the smooth gray surface. Even though there is only one position of minimum potential energy at the bifurcation, it is not considered convergent since any following movement of θ could cause an uncertain movement of the Pulley.

3) Bistable States: The last configuration in Fig. 3 is where there is no overlap between the Regions of Convergence. This means that the Pulley must be closer to the Link or the Tensioner, or in mathematical terms, k_R or k_E must be negative, repectively. Since the minimum energy of the system is where the cable is shortest, a straight line from the Tensioner to the end of the Link passes through the Rotator at two distinct points, corresponding to two "bistable states" of equal minimum energy.

This phenomenon can also be referenced to Fig. 4. For a given configuration in the bistable area, one position of minimum potential energy is located on one of the red flaps, and the other is located on the smooth gray surface. The amount of these bistable states decrease as $R_L : R_P$ increases since the Region of Convergence increases, making overlap more common. The bistable states will disappear as both $R_L : R_P$ and $R_P : R_T$ reach infinity.

The bistable states are not considered convergent since there are multiple equilibria (injective). However, if the Link is under control, the phenomenon of bistable states means that the Pulley will settle to either of two equilibria it is closest. Up to this point, it has been shown that the backdrivable system will converge to a single equilibrium point if both the Link-Pulley ($\theta - \phi$) and the Pulley-

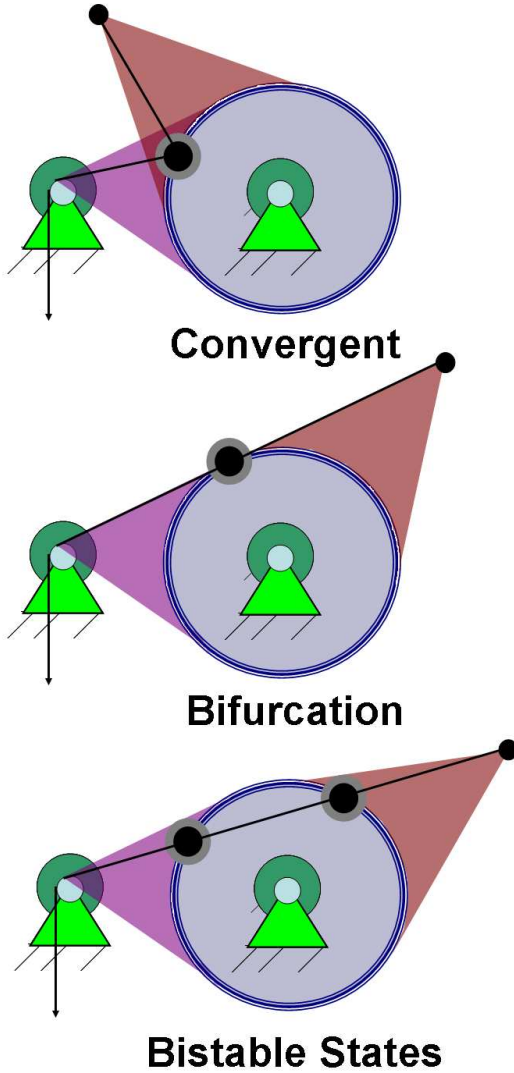**Convergent**

Bifurcation

Bistable States

Fig. 3. Three configurations are shown. The convergent case (Top) has overlapping Regions of Convergence, illustrated with the colored triangles. The Regions of Convergence border each other during a bifurcation (middle). The mechanism has two equilibria (bistable states - bottom) where the Regions of Convergence are out of phase.

Tensioner $(\phi - \zeta)$ relationships are within their respective Regions of Convergence. However when these regions do not intersect, the Pulley settles to either of two equilibria. Where the regions border each other (bifurcation), the subsequent motion of the Pulley is uncertain if the Link changes position.

These relationships would change drastically if, like in the version of the MARIONET introduced in a previous study [3], a mechanical advantage such as a block and tackle was implemented on either section of the cable (L_{LP} or L_{PT}). In this final section of analysis, the effects of this mechanical advantage are explored, with results that are quite unique.

C. Effect of Mechanical Advantage

Since the purpose of the MARIONET is to exert torque on the Link, a block and tackle with a mechanical advantage of
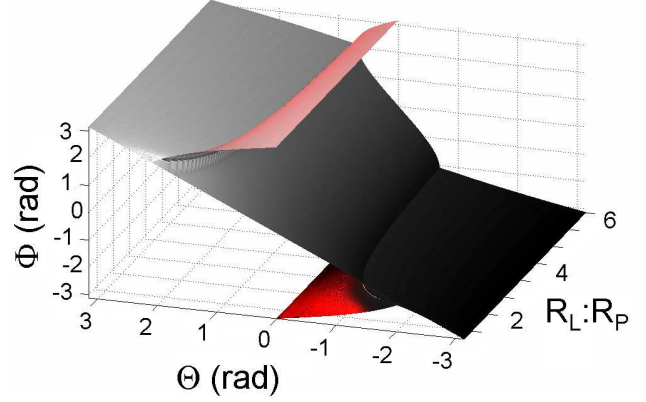

Fig. 4. Minimum energy surface for backdrivable, passive Rotator. This equilibria surface shows both the convergent region (outside the red flaps) and a bistable area (within the red flaps) where there are two equilibria for a given configuration. The intersection of the flaps with the surface indicates the bifurcation point. Note θ and ϕ are S^1 projected on an $\Re^1$.

4:1 amplifies the effect of the Tensioner in the present version previously mentioned. In the following, we will explore two separate cases: the first with a theoretical mechanical advantage of 1.1:1, and the second, the MARIONET's advantage previously indicated. The equations behind the device change slightly, where an amplification A multiplies the length of cable to which it is applied, in this case, L_{LP}. For purposes of brevity, only the torque on the Rotator will be shown here as an example:

$$\tau_R = A\frac{R_L R_P}{L_{LP}}\sin\left(\theta - \phi\right)T + \frac{R_P R_T}{L_{PT}}\sin\left(\phi - \zeta\right)T, \quad (12)$$

where A amplifies the effect of torque produced by L_{LP}.

The effect on the equations have interesting effects on the minimum energy surface shown in Fig. 5 for an $A = 1.1$. In this figure, where before the flaps extended all the way to the smooth, main surface, this case shows a gap. This is because at the location of bifurcation shown in the previous case, now there is a greater advantage to one side of the Rotator when the Regions of Convergence border each other. This means that once the configuration is on the main surface, it stays there unless the configuration is manually changed back to one of the flaps. This result is interesting because the mechanism acts as a type of switch, mathematically known as a "catastrophe". However, where catastrophe machines like the Zeeman machine can approach the cusp region multiple times, this configuration can only reach the region once. Thus, this specific type of catastrophe will be known as a *unidirectional bifurcation*.

The phenomenon of the "floating flaps" reduces as the mechanical advantage grows. Fig. 6 and Fig 7 show the minimum energy surfaces for mechanical advantages of $A = 2$ and that of the MARIONET ($A = 4$). This result is due to the first term in (12) (the weighted term), overpowering
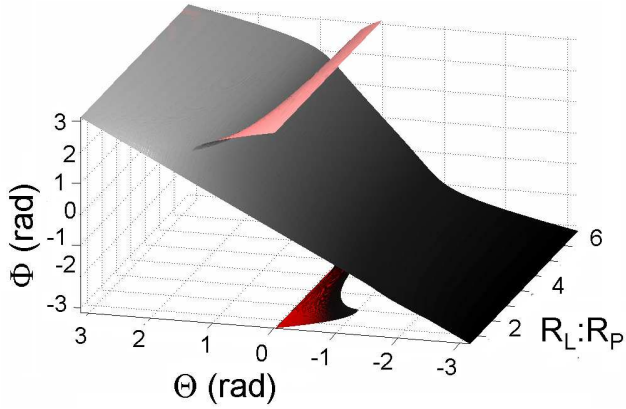
Fig. 5. Minimum energy surface with a theoretical mechanical advantage (block and tackle) amplification of $A = 1.1$.
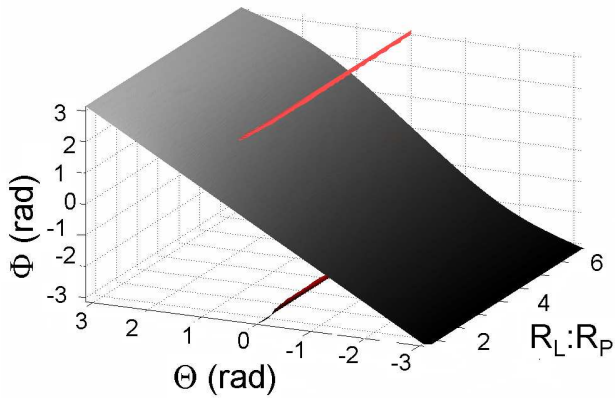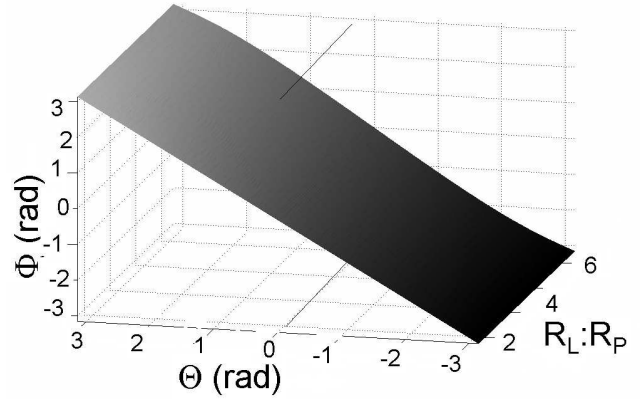

Fig. 7. Minimum energy surface with $A = 4$. This is the configuration of the present version of the MARIONET. The flaps have now reduced to thin lines indicating singularities.

Fig. 6. Minimum energy surface with $A = 2$.

the second term as the mechanical advantage increases. As A rises, the flaps begin to disappear, and the distance the Pulley jumps during a catastrophe increases. Eventually, the flaps visually disappear, but remain at singularities such as the those mentioned previously ($\phi = \zeta = \theta + \pi$). Excepting these singularities, the entire minimum energy surface for the MARIONET in Fig. 7 is bijective. Therefore we can conclude that this device is inherently stable.

III. CONCLUSIONS AND FUTURE WORKS

A. Conclusions

Besides investigation of interesting mathematical occurrences of the MARIONET, the purpose of this work was to prove mathematically that this device, already simple and inexpensive, is also safe and easy to control - fulfilling the needs in human-interactive devices. There are a number of more specific conclusions obtained. First, if the Rotator is non-backdrivable, the Link will always converge to a single equilibrium point at the Pulley. Second, if the Link is controlled but the Rotator becomes passive, the Pulley may

settle to either of two equilibria for portions of its workspace, and for other portions settle to a single equilibrium. The locations of this behavior can be mathematically determined by identifying the sign of the stiffness for both sections of cable. Finally, applying a mechanical advantage to one of the sections of cable has the effect of overpowering the other section, and creating what is identified in this paper as a unidirectional bifurcation, whose area decreases as the advantage increases. This phenomenon can be classified in nonlinear dynamics as a type of "catastrophe", where a small change in outside circumstances creates a large change in internal configuration. In the case of the MARIONET, this means that the Rotator jumps when the Link reaches a given location.

B. Future Works

While the current design of the MARIONET is an inherently stable mechanism with no catastrophes in its workspace, perhaps there are applications outside of rehabilitation and human motor control for a device that has unidirectional bifurcations. Catastrophe machines occur quite commonly in everyday use in the form of snaps and switches. Perhaps outside research can use a modified version of the MARIONET in such a way.

IV. ACKNOWLEGEMENTS

REFERENCES

[1] E.A. Jackson, *Perspectives of Nonlinear Dynamics*, Cambridge University Press, 1991.
[2] Woodcock, A.E.R. and T. Poston. *A geometrical study of the elementary catastrophes.* New York, Springer-Verlag, 1973.
[3] J.S. Sulzer, M.A. Peshkin and J.L. Patton, "MARIONET: An Exotendon-Driven Rotary Series Elastic Actuator for Exerting Joint Torque", *IEEE-International Conference on Rehabilitation Robotics (ICORR)*, Chicago, IL June 2005.